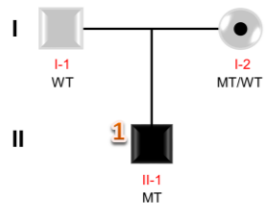
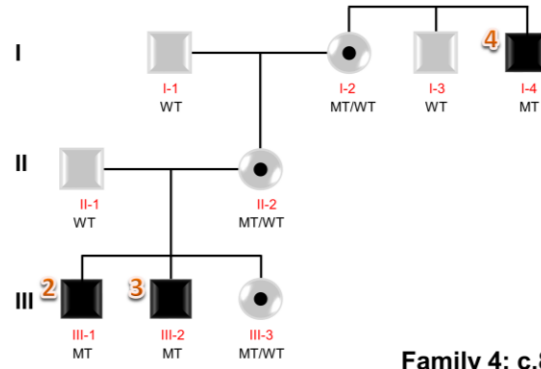


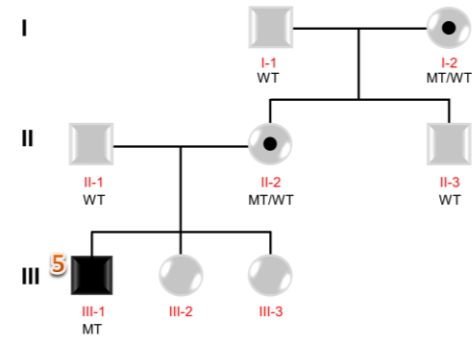
**Family 1: c.538-2A>G
p.(Asp180Valfs*5)**



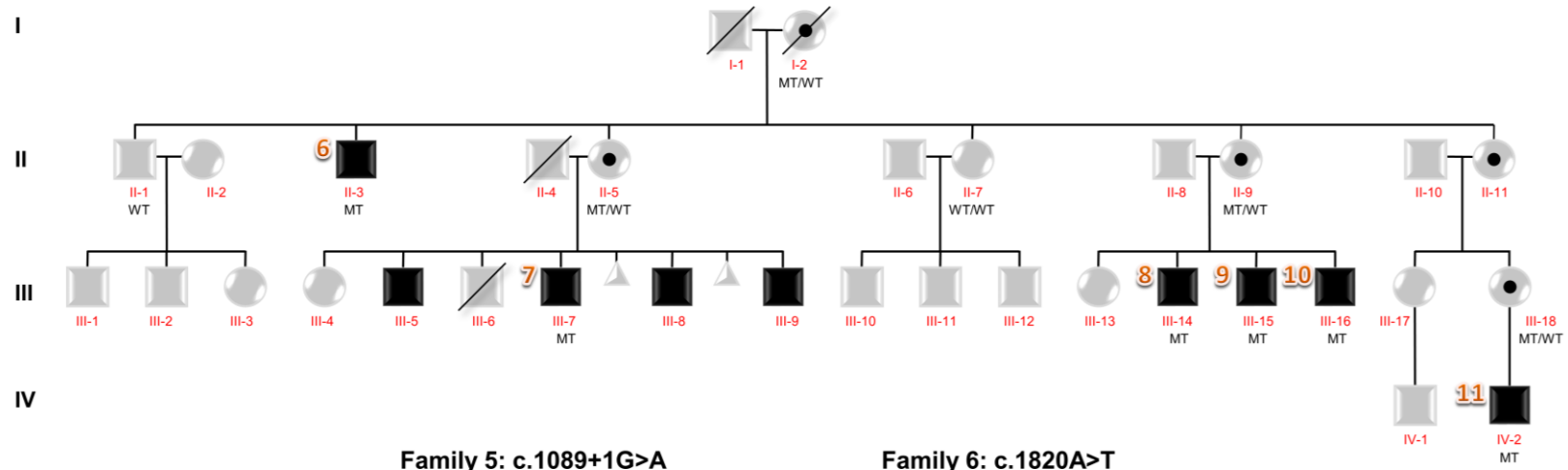
**Family 2: c.611C>G
p.(Pro204Arg)**



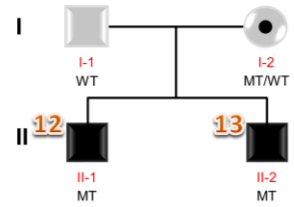
**Family 3: c.721C>T
p.(Arg241*)**



**Family 4: c.899T>C
p.(Leu300Ser)**



**Family 5: c.1089+1G>A
p.(Gly364Ilefs*10)**



**Family 6: c.1820A>T
p.(Glu607Val)**

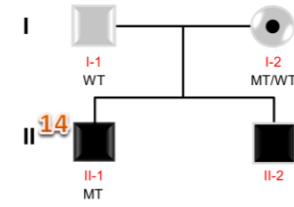


Figure S1. Pedigrees of six families with a *WNK3* variant. Affected and unaffected individuals are indicated respectively by black and pale grey squares or circles. When sequencing was done, the genotype (using MT for variant allele and WT for wild type allele) is indicated below the symbol of the individual. The number of each affected individual participating in the study is indicated by numbers written in red and bold larger fonts. VAF means variant allele fraction.

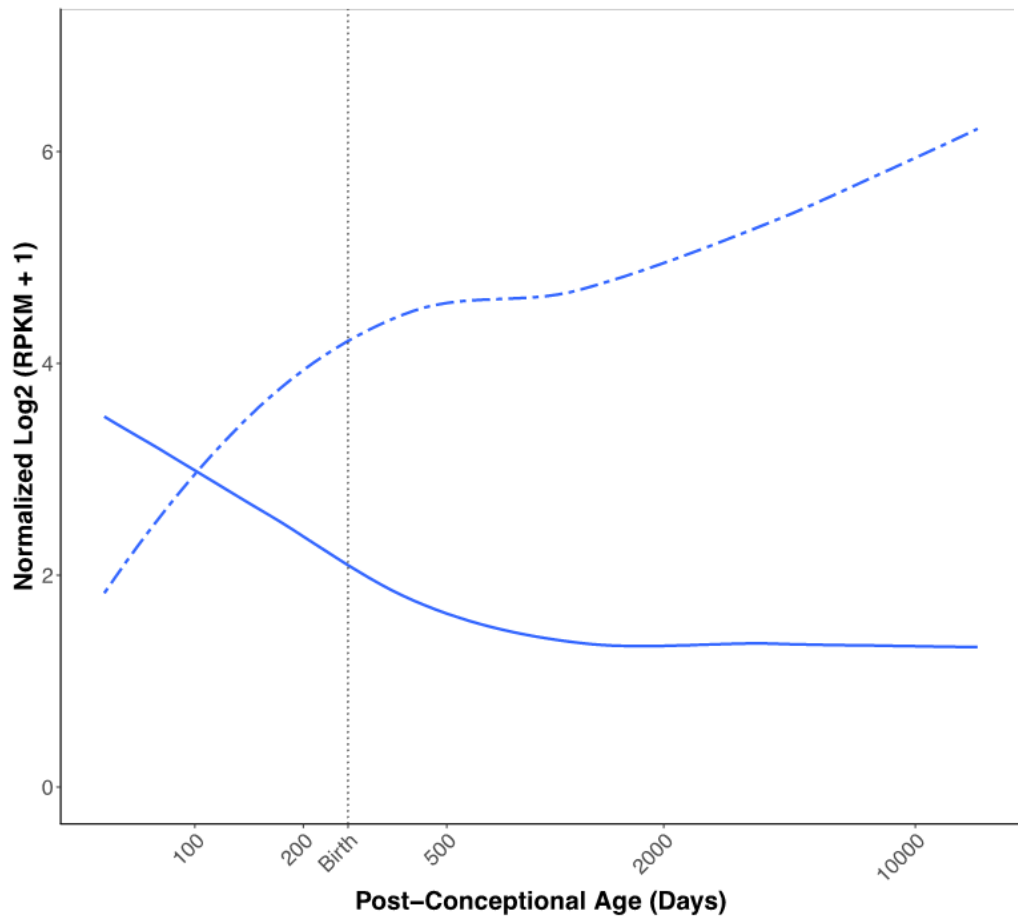
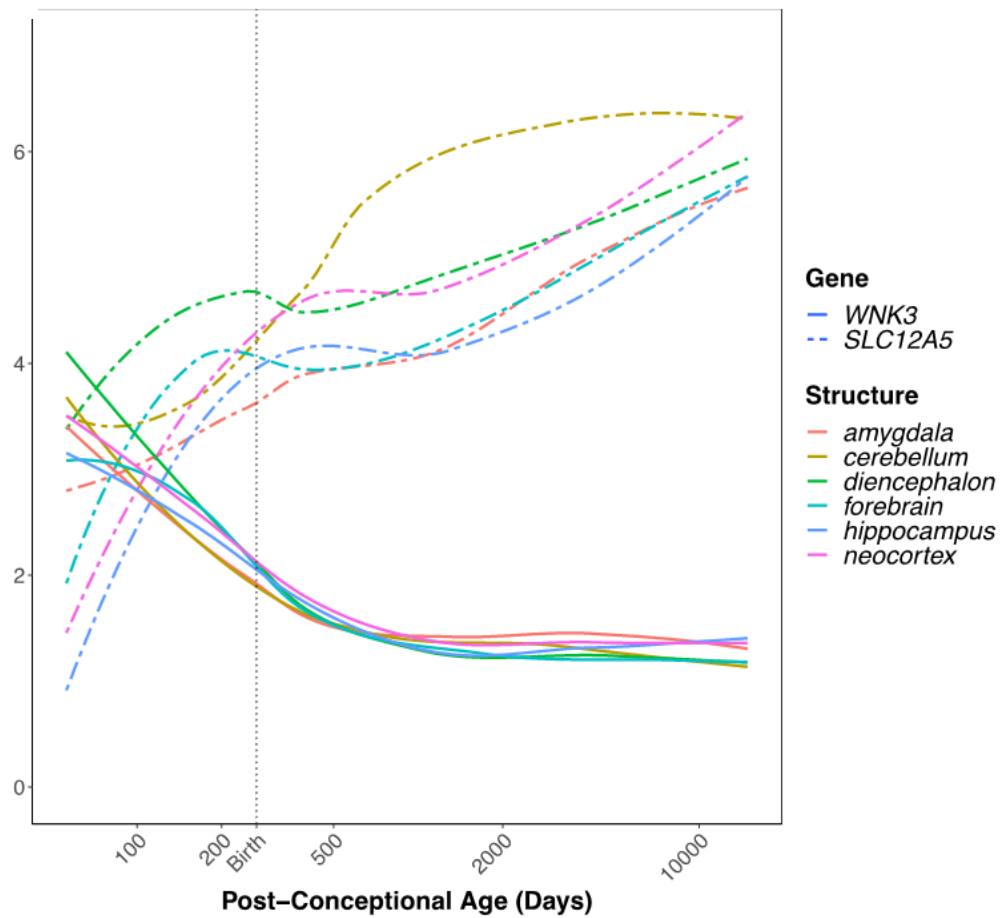
a**b**

Figure S2: Expression profiles of *WNK3* and *SLC12A5* (encoding KCC2) from BrainSpan (www.brainspan.org) Developmental Transcriptome¹. **a.**, Overall expression profiles of *WNK3* and *SLC12A5* are plotted as smoothed conditional means of expression over time. *WNK3* demonstrates decreased expression over time, while *SLC12A5* demonstrates increased expression over time. **b.**, Expression profiles of *WNK3* and *SLC12A5* are plotted as smoothed conditional means of expression over time stratified by regions.

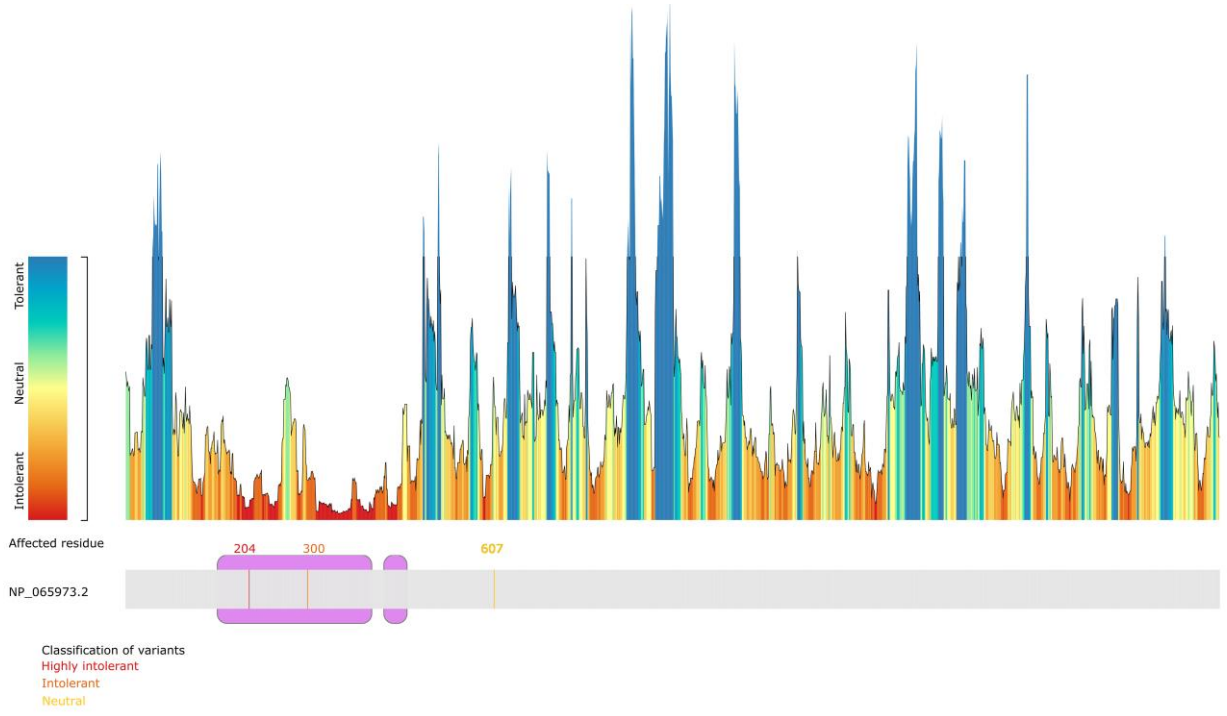
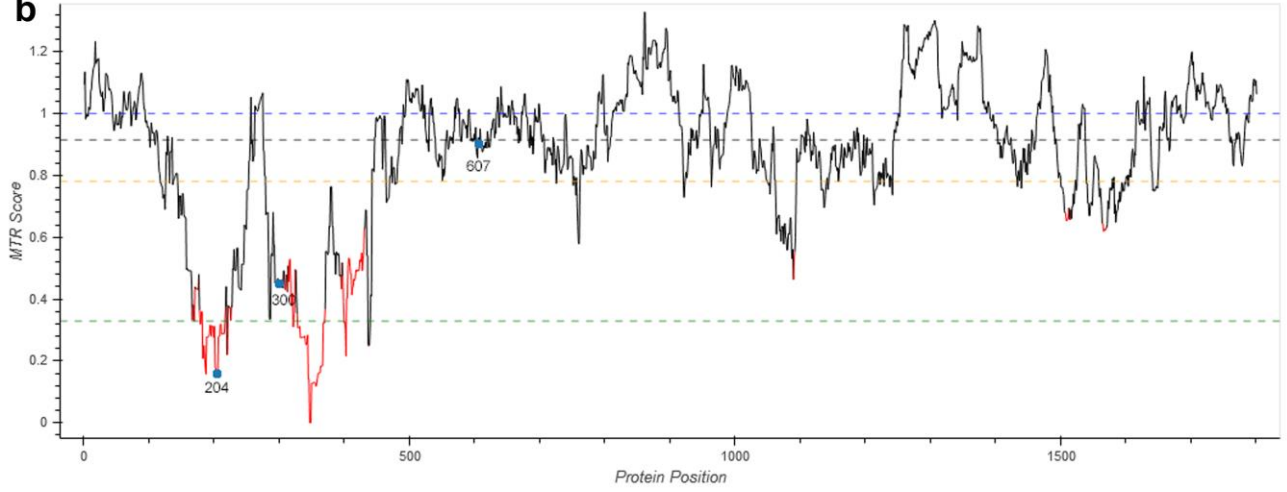
a**b**

Figure S3. Tolerance predictions of the amino acid residues of WNK3 (NP_065973.2) affected by the variants reported in the study. a., MetaDome web tool² indicates heterogeneous tolerance of WNK3 regions, inducing a classification of the residues of interest from highly intolerant to neutral to missense variants. The catalytic domain is globally the most intolerant region to missense variants. **b.**, Analysis by Missense Tolerance Ratio (MTR; v1)³ suggests that variants affecting intolerant residues 204 and 300 in the catalytic domain are expected to bear a severe effect on WNK3 function. Horizontal lines show gene-specific MTR percentiles 5th (in green), 25th (in yellow), 50th (in black), and neutrality (in blue; MTR = 1.0) MTR calculated using WES component of gnomAD v2.0.

NM_001002838.3(WNK3):c.1089+1G>A

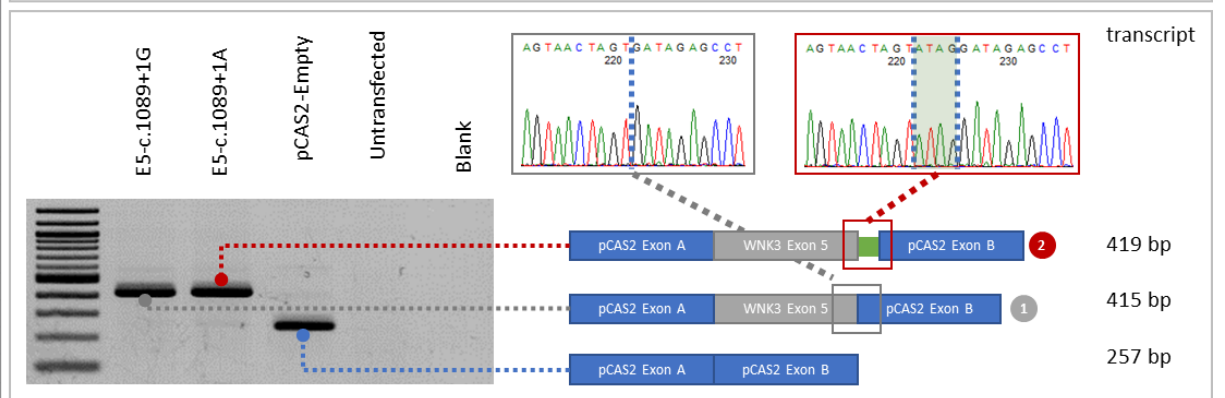
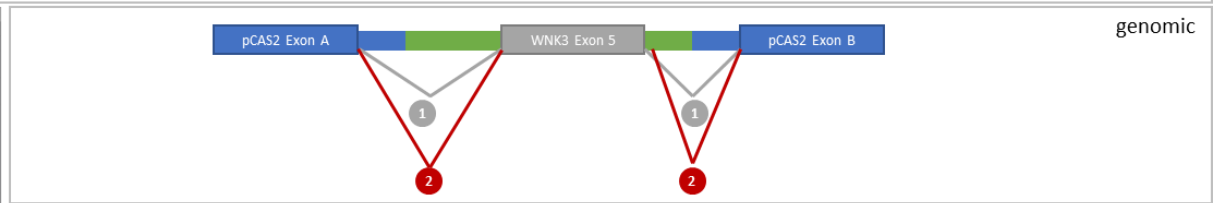
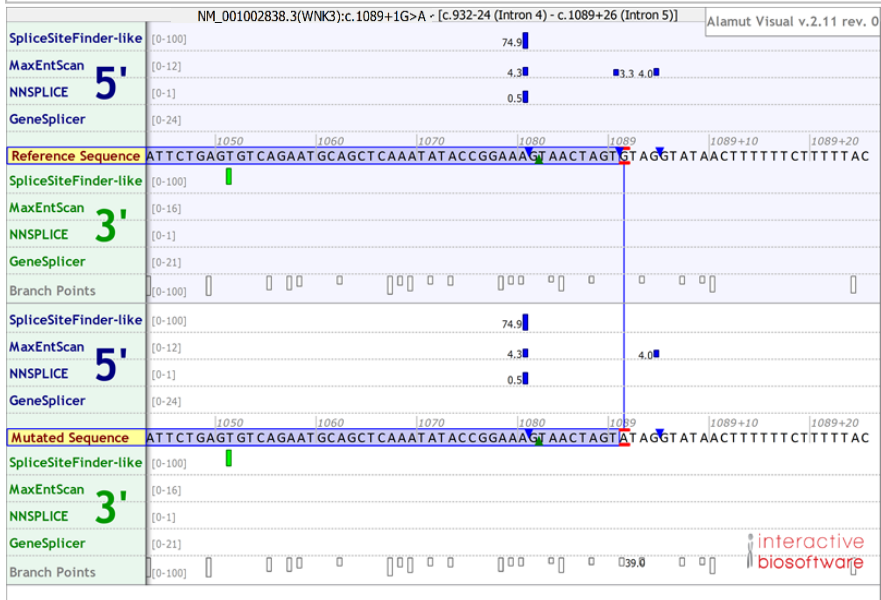


Figure S4. Assessment of the effect on splicing of variant c.1089+1G>A by mini-gene assay. To evaluate the impact on splicing of the NM_001002838.3(*WNK3*):c.1089+1G>A variant identified in individuals 12 and 13 (Family 5), in the absence of available biological samples, we performed mini-gene reporter assays using the pCAS2 vector based on a previously described protocol⁴. This functional assay is based on the comparative analysis of the splicing pattern of wild-type and mutant. Mini-gene constructs of the exon 12 reveal two different transcripts. The wild-type construct (E5-c.1089+1G) highlights the transcript 1 (415 base pairs (bp)) corresponding to the physiological splicing of the exon 5. However mutant construct (E5-c.1089+1A) presents predominantly the transcript 2, four bp longer than transcript 1. This is due to the recruitment of an alternative donor site in exon, 5 located 4 bp 3'-downstream to the physiological splice site. This results in a reading frame shift and the occurrence of a premature stop codon p.(Gly364Ilefs*10).

DNA variants are described according to the nomenclature established by the Human Genome Variation Society. Nomenclature HGVS V2.0 is defined according to *WNK3* mRNA reference sequence NM_001002838.3. Nucleotide numbering uses +1 as the A of the ATG translation initiation codon in the reference sequence, with the initiation codon as codon 1.

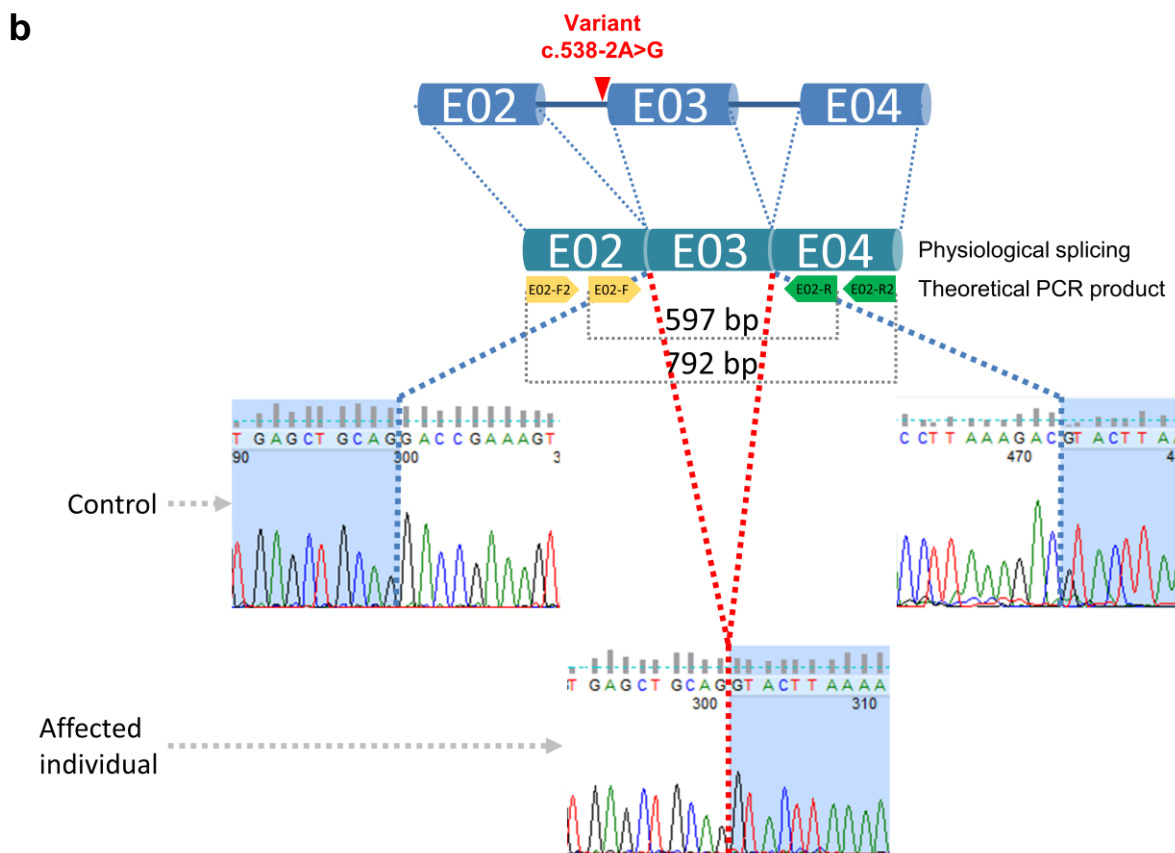


Figure S5. Assessment of the effect on splicing of variant c.538-2A>G by RNA analyses.

To evaluate the impact on splicing of the NM_001002838.3(*WNK3*):c.538-2A>G variant (intron 2), we performed a compared analysis of RNAs isolated from peripheral blood samples collected in individual 1 and in a healthy control having a wild-type *WNK3* sequence, respectively. For both affected and healthy individuals, we did a nested-PCR amplification of the region containing the exon junctions predicted to be affected by the splice site according to prediction programs, as shown in the screenshot from Alamut software (Sophia Genetics) (**a**). We thus designed two forward primers in exon 2 (E02F and E02F2) pairing two reverse primers located in exon 4 (E02R and E02R2) and sequenced the PCR products by Sanger sequencing (**b**). Whereas normal splicing in the control was objectified by the presence of exon 3 sequence, skipping of exon 3 was confirmed in individual 1 by a direct junction between exons 2 and 4 leading to a frameshift and a premature stop codon five codons downstream [p.(Asp180Valfs*5)].

DNA variants are described according to the nomenclature established by the Human Genome Variation Society. Nomenclature HGVS V2.0 is defined according to *WNK3* mRNA reference sequence NM_001002838.3. Nucleotide numbering uses +1 as the A of the ATG translation initiation codon in the reference sequence, with the initiation codon as codon 1.

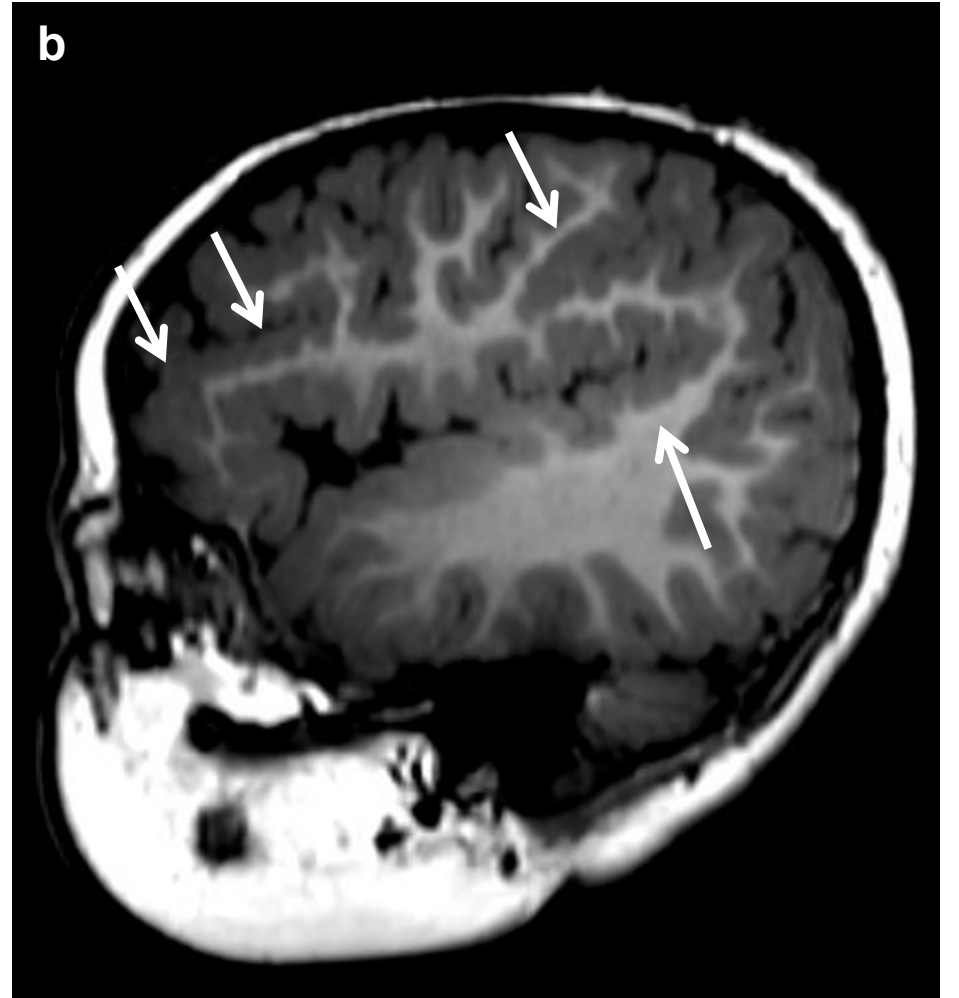


Figure S6. Brain imaging of affected brothers from Family 2 [variant NM_001002838.3(WNK3):c.611C>G p.(Pro204Arg)]. MRI scans from individuals 2 and 3 (Family 2). **a.**, MRI of individual 2, imaged at 5 years of age. Axial image from 3D T1 MRI sequence demonstrates areas of perisylvian polymicrogyria (white arrows) as well as multiple foci of bilateral periventricular grey matter heterotopia (orange arrows); **b.**, MRI of individual 3 at 19 months of age. Sagittal image from 3D T1 sequence showing areas of frontal and perisylvian polymicrogyria (white arrows).

References

1. Kang HJ, Kawasaki YI, Cheng F, et al. Spatio-temporal transcriptome of the human brain. *Nature*. 2011;478(7370):483-489.
2. Wiel L, Baakman C, Gilissen D, Veltman JA, Vriend G, Gilissen C. MetaDome: Pathogenicity analysis of genetic variants through aggregation of homologous human protein domains. *Hum Mutat*. 2019;40(8):1030-1038.
3. Traynelis J, Silk M, Wang Q, et al. Optimizing genomic medicine in epilepsy through a gene-customized approach to missense variant interpretation. *Genome Res*. 2017;27(10):1715-1729.
4. Soukarieh O, Gaildrat P, Hamieh M, et al. Exonic Splicing Mutations Are More Prevalent than Currently Estimated and Can Be Predicted by Using In Silico Tools. *PLoS Genet*. 2016;12(1):e1005756.